Semiconductor Physics, Quantum Electronics & Optoelectronics, 2005. V. 8, N 1. P. 53-59.

PACS: 73.61Ga, 61.72Vv, 61.80.Jh, 66.30Jt

Effect of internal electrical field on compositional dependence of *p-n* junction depth in ion milled *p*-$Cd_xHg_{1-x}Te$

I.I. Izhnin[1], V.V. Bogoboyashchyy[2], K.R. Kurbanov[3], K.D. Mynbaev[4], V.M. Ryabikov[5]

[1] *R&D Institute for Materials SRC "Carat", 202 Stryjska Str., 79031 Lviv, Ukraine*
[2] *Kremenchuk State Polytechnical University, 20, Pershotravneva Str., 39614 Kremenchuk, Ukraine*
[3] *Institute of Economy and New Technology, 24/37, Proletarska Str., 39600 Kremenchuk, Ukraine*
[4] *Ioffe Physico-Technical Institute, St.Petersburg, 194021 Russia*
[5] *JSC Pure Metals, 3, Zavodska Str., 27500 Svitlovodsk, Ukraine*

Abstract. The dependence of the conversion depth in $Cd_xHg_{1-x}Te$ alloys subjected to ion-beam milling (CMT) on alloy composition and treatment temperature is studied both experimentally and theoretically. It is shown that in compositionally homogeneous crystals the dependence is defined by internal electric fields, which affect the diffusion of charged intrinsic defects that arise as a result of the treatment. The results of calculations of the effect of the potentials of the *p-n* junction formed by ion-milling on the conversion depth fit well both the original experimental data and those taken from the literature. The data obtained confirm the validity of the diffusion model of the formation of the excessive mercury source in CMT subjected to ion-beam milling, which was proposed by the authors earlier. The results gained allow one to precisely predict and control the conversion depth in CMT crystals and epitaxial layers subjected to ion milling for *p-n* junction fabrication. This makes the results presented in the paper useful in CMT infrared detector technology.

Keywords: $Cd_xHg_{1-x}Te$, ion-beam milling, conductivity type conversion.

Manuscript received 01.12.04; accepted for publication 18.05.05.

1. Introduction

Ion-beam milling (IBM) of narrow bandgap *p*-$Cd_xHg_{1-x}Te$ (CMT) alloys is currently an approved technique for *p-n* junction fabrication in CMT infrared detector technology [1, 2]. The method is based on the phenomenon of the formation of a thick surface layer with *n*-type conductivity in an undoped *p*-type CMT crystal with $\sim 10^{16}$ cm^{-3} Hg vacancies subjected to IBM [3]. It is commonly accepted now that deep *p*- to *n*-type conversion under IBM is due to the diffusion of excessive interstitial Hg atoms generated under ion milling. However, the exact mechanisms of defect interaction in the converted layer and the effect of external plasma are still under debate [4]; formation mechanism of the source of the excessive mercury is not understood either. Some authors believe that the interstitial Hg atoms come from a layer etched from the crystal surface during IBM. However, according to [5], in reality the sputtered atoms originate only from the depth of the first 2 – 3 atomic layers, which comprises a layer not thicker than 1 nm. Authors of Ref. [1] believed that about 0.02 % of mercury atoms released from the crystal lattice as a result of IBM are first implanted in the crystal down to the depth of 1 μm, and then move further via plasma-stimulated diffusion. Quite a different mechanism was suggested in Refs [6 – 8]. There, the generation of excessive mercury was explained using the mechanism based on the well-known model of a "thermal spike" [9]. According to [6 – 8], at the spot where the ion interacts with the surface, a microscopic melt area is formed. This area very quickly crystallizes, forming quite a few point defects in the cation sublattice. These defects annihilate with each other, however, some quick interstitial mercury atoms penetrate into the bulk of the crystal, where they diffuse via relay mechanism and interact with Hg vacancies and acceptor dopant atoms, causing conductivity type conversion. The very top CMT surface layer of 5 – 7 nm in thickness contains a lot of defects, is depleted with Hg and thus, has *p*-type conductivity.

Major features of *p-n* junction formation in CMT subjected to IBM have been recently reviewed in [4]. Several conclusions were made there. First, it is noted that in the majority of the IBM experiments the *p-n* junction depth *l* appears to be proportional to the square root of irradiation dose divided by the concentration of the excessive tellurium (or Hg vacancy concentration in case of homogeneous CMT) in the bulk of the crystal. At the same time, in Refs [1, 10] where conversion was studied in CMT epitaxial layers with a cap protective layer, *l* depended on this relation linearly.

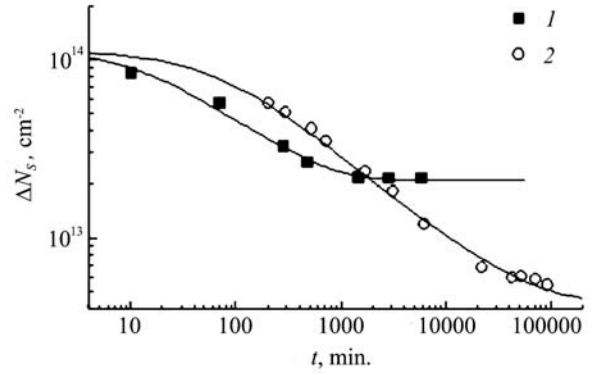

Fig. 1. The dependence of the IBM-induced increase in the electron concentration at 77 K, reduced to a sample area, on the time of the storage at 300 K for the samples: 1 – P17-1, 2 – P22-1.

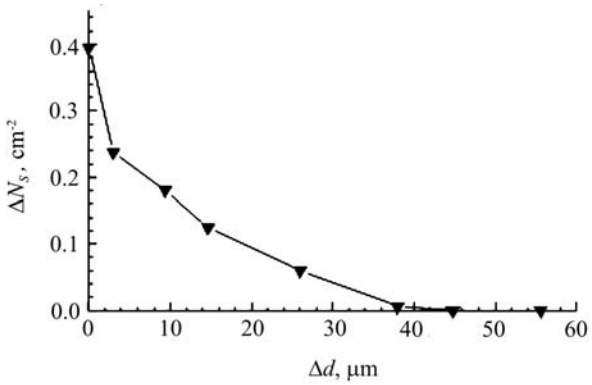

Fig. 2. The dependence of the IBM-induced increase in the electron concentration, reduced to a sample area, for the sample P18-1 after storage, on the thickness of the removed layer.

Secondly, a number of experiments revealed a complex two-layer structure of the converted *n*-type layer. In CMT with $x = 0.2$ after IBM, the top (surface) layer up to 3 μm in thickness demonstrated the high electron concentration (10^{17}...10^{18} cm^{-3} at 77 K) with the mobility of the order of about 10^4 cm^{2}V^{-1}s^{-1}. The inner layer was homogeneous with the electron concentration and mobility of about 10^{15} cm^{-3} and 10^5 cm^{2}V^{-1}s^{-1}, respectively. According to [1], the top layer comprises a 0.5…1 μm-thick radiation-damaged layer and a 2…3 μm-thick second layer, in which the electron concentration decreases exponentially from the surface. Actually, radiation-induced damages, such as dislocation loops located at ~ 50 nm below the surface have been observed in CMT after IBM by transmission electron microscopy [11].

Yet another feature of IBM-induced conversion in CMT, according to [4], was a strong dependence of the conversion depth l on the alloy composition x. While in narrow bandgap CMT with $x = 0.2$ l may reach hundreds of micrometers [12], it quickly decreases with x increasing, so at $x > 0.4$ the conversion takes place only in a very thin surface layer [4]. This observation is especially important since in modern CMT technology it became a custom to cap free CMT surface with a thin (~1 μm) wider bandgap protective layer [1, 4]. A drastic decrease of l in CMT capped with such a layer has been observed experimentally in [13].

The drastic decrease of l with increasing x is difficult to interpret, if one believes that a source of Hg atoms is the layer milled by the ions from the surface. In contrast to this, the effect of x on l can be easily understood, when a drift of charged interstitial mercury in electric field originating at the interface between the very top *p*-type defect layer and converted *n*-type layer is considered, according to the model suggested in [6 – 8]. As the strength of the field increases with x increasing, the conversion depth should decrease.

In this work, we report on experimental studies of the conversion depth dependence in CMT under IBM on the alloy composition, and correlate the experimental results with those of theoretical calculations that model the effect of the internal electric field on the process of conversion at different temperatures. Calculations were performed within the frames of the model [6 – 8]. The results obtained confirm experimentally the validity of the diffusion mechanism of Hg source formation in CMT subjected to IBM, as proposed in [6 – 8].

2. Experiment

We have studied homogeneous single-crystal vacancy-doped *p*-type CMT wafers with $x = 0.16…0.28$. The crystals were grown using elemental Hg, Cd, and Te with 6N class of purity at "Pure metals" factory (Svitlovodsk, Ukraine) by vertical-directed crystallization with replenishment from the solid phase. They were doped with In, which ensured *n*-type conductivity of the wafers with concentration $N_D - N_A \approx 3 \cdot 10^{14}$ cm^{-3} after IBM or low-temperature annealing at Hg-saturated conditions. After the growth, the wafers were annealed at 410 °C in Hg vapors to obtain *p*-type conductivity with the mercury vacancy concentration of 10^{16} cm^{-3}. The vacancy concentration was determined by measuring the hole concentration at 77 K. The measurements comprised investigations of field dependences for the Hall coefficient and conductivity, as well as processing the experimental data using the Mobility Spectrum Analysis (MSA) method [14] with consideration for the degree of vacancy ionization at 77 K as depending on their concentration and alloy composition [15, 16]. Parameters of the samples are given in Table.

IBM milling was performed with Ar^+ ions possessing the energy 500 eV, ion current density $j = 0.2$ mA/cm^2 and treatment duration $t = 200$ s. The temperature of the samples during IBM was either 293 K (water cooling of sample holder) or 345…350 K (no cooling).

The *p-n* junction depth was determined either by measuring the Hall coefficient and conductivity of the

Sample parameters

Sample	x	$p_{77}\cdot10^{-16}$, cm^{-3}	$[V_{Hg}]\cdot10^{-16}$, cm^{-3}
P16-1	0.202	1.47	1.30
P17-1	0.162	2.40	2.30
P18-1	0.206	1.21	1.04
P19-1	0.212	1.31	1.22
P20-1	0.242	0.78	0.71
P21-1	0.228	1.16	1.12
P22-1	0.276	0.64	0.72

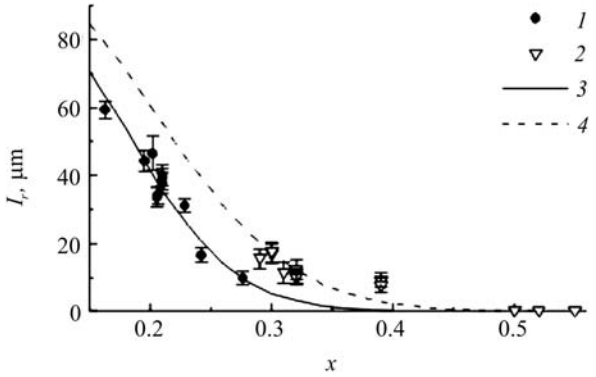

Fig. 3. The calculated dependence of the reduced conversion depth on the alloy composition for $T = 293$ K (1) and 345 K (2). Points designate experimental data from: 3 – this work, 4 – Ref. [4].

samples with step-by-step chemical etching, or using scanning electron microscopy in electron beam induced current mode. To ensure time relaxation of IBM-induced defects after the IBM, the samples were stored for two months at room temperature. During the storage, the Hall coefficient and conductivity of the samples were periodically measured in various magnetic fields, and being based on these data the electron and hole concentrations at 77 K were determined using the MSA method. Fig. 1 demonstrates an IBM-induced increase in the concentration of electrons ΔN_S with the mobility $\sim 10^5$ $cm^2V^{-1}s^{-1}$, as measured at 77 K and reduced to a sample area. The data are given for samples P17-1 and P22-1 that represent the specimens with the lowest and highest alloy composition x, respectively. It is seen from the figure that the initial ΔN_S value did not depend on x and comprised $\sim 10^{14}$ cm^{-3}; this value corresponds to that typical of a radiation-damaged layer. With the storage time t_{st} increasing, ΔN_S was decreasing as $1/\sqrt{1+t_{st}/\tau}$ with $\tau \sim 10^3 \ldots 10^4$ s, and reached saturation at $t_{st} > 10^3 \ldots 10^4$ min. Such behavior of ΔN_S corresponds to donor disintegration by a 3rd-order reaction. The fact of n^+ layer relaxation was confirmed by the results of electrical measurements with step-by-step chemical etching, performed with the crystals after the storage. Fig. 2 shows the dependence of ΔN_S on the thickness of a chemically etched layer for the sample P18-1. It is seen that the damaged layer after $\sim 10^5$ min of storage retained only $\sim 1-2$ % of the initial donor concentration; at the same time, ΔN_S did not exceed the value $3\cdot10^{12}$ cm^{-2} in the bulk of *n*-layer.

The measured values were used to calculate the *p-n* junction depth l_r reduced to the vacancy concentration $[V_{Hg}]_0 = 10^{16}$ cm^{-3} and the ion fluence $\Phi_0 = 10^{18}$ cm^{-2}:

$$l_r = l\sqrt{\Lambda\frac{[V_{Hg}]}{\Phi}}, \qquad (1)$$

where $\Lambda = \Phi_0 / [V_{Hg}]_0 = 1$ m is a characteristic ratio; $\Phi = jt/e$.

The experimental data are shown in Fig. 3. It is seen there that the junction depth increases with temperature increasing and decreases with x increasing.

3. Modeling

The proposed in this work model proceeds from the assumption of the diffusion nature of excessive mercury source as suggested in [6 – 8]. According to [5], CMT etching with ions possessing ~ 1 keV energy sputters only 2 to 3 atomic surface layers. Thus, the energy imparted to a crystal by ions is mostly transferred into heat [6], which leads to the formation of a microscopic melt area, i.e., a thermal spike of $V_{min} \sim 10^{-19}$ cm^{-3} in the volume and with the length L within the limits 5 to 7 nm. Due to the very small value of V_{min}, melt crystallization and thermal relaxation of the thermal spike last less than 10^{-12} s [6]. Thus, after cooling down, the spike area contains quite a few ($N_0 \sim 10^{22}$ cm^{-3} [6]) non-equilibrium defects, the majority of them being doubly ionized mercury interstitials ($Hg_I^{\bullet\bullet}$) and vacancies (V_{Hg}''), as well as neutral vacancy complexes, most probably bivacancies ($W_{Hg}^{\times}$). During relaxation of these defects by means of mutual annihilation, which lasts $t_{rel} \sim 10^{-9}$ s [8], some interstitials penetrate from the defect layer into the crystal bulk, thus forming a diffusion source of excessive mercury at the external border of the conversion layer. The interstitials further diffuse from this source into the bulk of the crystal and annihilate with mercury vacancies, causing *p*-to-*n* conductivity type conversion.

Due to the fact that mercury atoms move from the thermal spike area into the crystal, as well as to preferential mercury evaporation during IBM of CMT [5], the defect layer, which is the very thin surface layer with the thickness $L = 5 \ldots 7$ nm, is strongly depleted with mercury. According to [8], 98 % of this mercury deficiency exist in the form of neutral mercury bivacancies, which interact with $Hg_I^{\bullet\bullet}$ much weaker than ionized single vacancies V_{Hg}''. The maximum mercury

deficiency δ_0 in the defect layer is reached when this layer becomes impermeable for $Hg_I^{\bullet\bullet}$. This condition is reached when $\delta_0 = 10^{19}$ cm^{-3}. Therefore, the defect layer contains $0.02\delta_0$ (i.e., $\sim 2\cdot10^{17}$ cm^{-3}) uncompensated V_{Hg}'', which define its *p*-type conductivity [6, 8]. As a result, a *p-n* junction occurs at the interface between the defect layer and the conversion one. Electric field of this junction hinders $Hg_I^{\bullet\bullet}$ from penetrating into the crystal.

As the defect layer is impermeable for $Hg_I^{\bullet\bullet}$, the etched-out region (the top 1 nm of the layer [5]) cannot act as a source of $Hg_I^{\bullet\bullet}$. Hence, the inner part of the defect layer with a thickness of $\sqrt{D_I t_{\text{rel}}} \approx 1$ nm, where D_I is the diffusion coefficient of $Hg_I^{\bullet\bullet}$ in the bulk of the sample at the milling temperature. The average $Hg_I^{\bullet\bullet}$ concentration in the source is [8]:

$$c_{I0} = \frac{jS}{4\pi e D_I r_w} \ln\left(1+\frac{N_0}{\delta_0}\right). \qquad (2)$$

Here S is the effective area of the thermal spike cross-section; N_0 is the initial concentration of $Hg_I^{\bullet\bullet}$ in a thermally relaxed thermal spike, $r_w = a/\sqrt{2}$ is the caption radius for $Hg_I^{\bullet\bullet}$ on a neutral Hg bivacancy, and $a = 0.648$ nm is the CMT crystal lattice parameter.

To calculate the conversion depth as a function of CMT characteristics and IBM parameters, let us consider a semi-bounded crystal with a flat surface. The coordinate z will be directed along the inner normal to the surface, while the reference point $z = 0$ will coincide with the interface between the defect layer and the conversion one. If so, the surface of the crystal is located at $z = -L$, where L is the thickness of the defect layer, and the interface between the conversion layer and the *p*-type "core" of the crystal is located at $z = l$. Within the frames of the above listed assumptions, the density of the diffusion flux of Hg at $z = l$ according to [8] is

$$J_{\text{Hg}} = D_I c_{I0} \left\{ \int_0^l \exp\left[\frac{2e\Delta\varphi(z)}{k_B T}\right] dz \right\}^{-1}; \qquad (3)$$

subject to $l >> r_0$, where r_0 is the Debye screening length. Here $\Delta\varphi = \varphi(z) - \varphi(0)$; φ is an electric field potential of the structure.

The conversion depth l as a function of IBM duration t can be calculated considering the conservation law for the amount of matter at the inner boundary of the conversion layer $z = l$, which appears as [6]:

$$\Delta_{\text{tr}}\, dl = J_{\text{Hg}}\, dt, \qquad (4)$$

where Δ_{tr} is the density of caption centers for $Hg_I^{\bullet\bullet}$ in an initial CMT crystal. In particular, in homogeneous vacancy-doped CMT crystals $\Delta_{\text{tr}} = [V_{Hg}'']$. Upon integration of the Eq. (4) considering (2, 3), we get the following equation:

$$\int_0^l (l-z)\exp\left[\frac{2e\Delta\varphi(z)}{kT}\right] dz = \frac{\Phi S}{4\pi r_w \Delta_{\text{tr}}} \ln\left(1+\frac{N_0}{\delta_0}\right). \qquad (5)$$

Solving the Eq. (5) requires to calculate the distribution of the potential φ in the structure. At $l >> r_0$ and $(4\pi/3)N_I r_0^3 << 1$, where N_I is the charged center concentration in the diffusion region, it can be found on the basis of the one-dimensional Poisson equation in the continuous approximation:

$$\frac{d^2\varphi}{dz^2} = \frac{4\pi e}{\varepsilon_S}(n - p - N). \qquad (6)$$

with $N = N_D - N_A$.

As the thickness of the defect layer L is of the order of the screening length, we calculated φ by solving (5) numerically. According to the above listed estimations for the vacancy concentration in the defect layer, we assumed that $N = 4\cdot10^{17}$ cm^{-3} at $-L < z < 0$. The donor concentration in the conversion layer ($z > 0$) was taken as $N = 1\cdot10^{15}$ cm^{-3}, which is a typical value of N in such an experiment. Since the $Hg_I^{\bullet\bullet}$ concentration in the conversion layer is small ($\sim 10^{12}\ldots10^{13}$ cm^{-3} [6 – 8]), these defects were not considered in (5). In accordance to [6], we assumed that $L = 6$ nm. The presence of the damaged layer and top *n*-layer enriched with donors was neglected as a first approximation. A possible influence of these layers will be discussed below.

The electron and hole concentration in (6) were calculated as

$$n = \int_0^\infty N_e(\varepsilon)\left[1+\exp\left(\frac{\varepsilon - e\varphi - F + E_C}{kT}\right)\right]^{-1} d\varepsilon; \qquad (7)$$

$$p = N_V \exp\left(-\frac{e\varphi + F - E_V}{kT}\right). \qquad (8)$$

The density of states $N_e(\varepsilon)$ was calculated using the well-known formula:

$$N_e(\varepsilon) = \frac{\sqrt{2}\, m_e^{3/2}}{\pi^2\hbar^3} \sqrt{\varepsilon\left(1+\frac{\varepsilon}{E_g}\right)} \cdot \left(1+\frac{2\varepsilon}{E_g}\right); \qquad (9)$$

where $m_e = \dfrac{m_0}{-\gamma_S + \frac{2}{3}\cdot\frac{E_p}{E_g}\left(1+\frac{1}{2}\cdot\frac{E_g}{\Delta_0+E_g}\right)}$ [17].

We assumed that $E_p = 17.3$ eV; $\gamma_S = 0.5$ [17]; $\Delta_0 = 0.96$ eV [18]. Here γ_S is a parameter that allows for the effect of remote bands similar to the Luttinger parameters; $E_p = 2m_0P^2/\hbar^2$. Calculations were performed using the empirical data from [19] for the density of states inherent to heavy holes N_V:

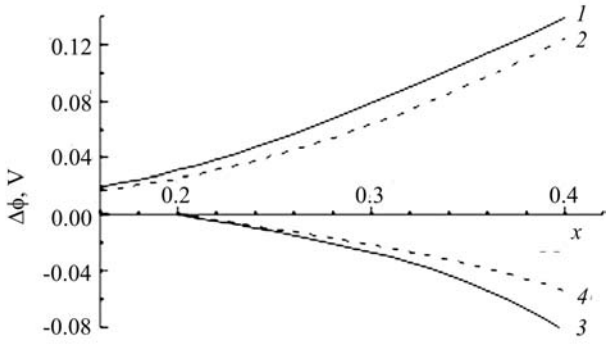

Fig. 4. The calculated dependence of the potential difference of the defect layer field (1, 2) and of the potential of a varyband protective layer (3, 4) on the composition of the protective layer in CMT structure with $x = 0.2$ at $T = 293$ K (1, 3) and 345 K (2, 4).

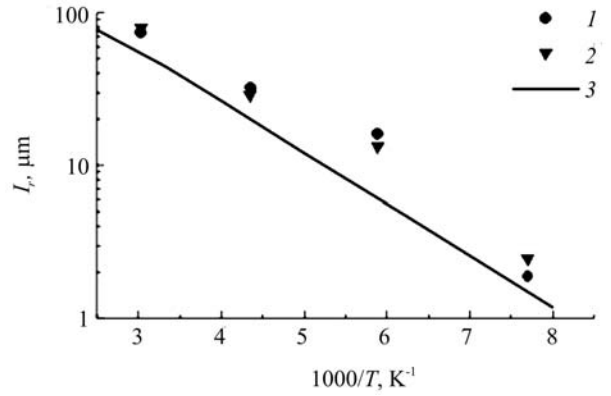

Fig. 5. Temperature dependence of the conversion depth, reduced to the vacancy concentration $1\cdot10^{16}$ cm^{-3} and ion fluence $1\cdot10^{18}$ cm^{-2}, in narrow bandgap CMT subjected to IBM. The points show experimental data from Ref. [12] for vacancy-doped CMT ($x = 0.21$) with the hole concentration $1\cdot10^{16}$ (1) and $5\cdot10^{15}$ cm^{-3} (2) at 77 K. Line 3 presents the results of calculations by the formula (12) for $x = 0.20$.

$$N_V = 2\left[\frac{m_{hh}k_B T}{2\pi\hbar^2}\right]^{3/2}\left[1+\frac{T}{T_1}+\left(\frac{T}{T_2}\right)^2\right]; \qquad (10)$$

where $T_1 = 334$ K and $T_2 = 594$ K are fitting parameters with the temperature dimensionality, $m_{hh} = 0.40m_0$ is the effective mass of heavy holes at $\varepsilon = 0$.

The bandgap value as a function of the temperature and alloy composition was calculated using the interpolation formula from [19]:

$$E_g(x,T) = -0.3098 + 1.9409x - 0.7351x^2 + 0.7061x^3 + 6.345\cdot10^{-4}T(1 - 2.195x + 0.309x^2 + 0.343x^3)\ \text{eV}. \qquad (11)$$

According to [19], (11) accounts for the temperature dependence of E_g better than other formulae, since it correctly considers the dependence of pre-exponential factor α_0 on E_g, temperature and population of states in the conduction band in Urbach's rule.

4. Results and discussion

Eq. (5) was solved in [6 – 8] for conductivity type conversion in compositionally uniform CMT subjected to IBM. According to obtained solution, the conversion depth is given as

$$l = l_0\sqrt{\frac{\Phi}{\Lambda\Delta_{tr}}}\exp\left(-\frac{e\Delta\varphi}{kT}\right); \qquad (12)$$

where

$$l_0 = \sqrt{\frac{\Lambda S}{2\pi r_w}\ln\left(1+\frac{N_0}{\delta_0}\right)}. \qquad (13)$$

Here $\Delta\varphi = \varphi(l) - \varphi(0)$ is the potential difference between internal ($z = l$) and external ($z = 0$) boundaries of the conversion layer.

It is seen that the factor l_0 defined by (12) and (13) is independent of the mercury interstitial diffusion coefficient D_I, because the $Hg_I^{\bullet\bullet}$ concentration in the diffusion source, according to (2), is inversely related to D_I. Hence, l_0 does not depend on the diffusion coefficient of $Hg_I^{\bullet\bullet}$, and therefore, on the temperature. The dependence of l_0 on the alloy composition is determined by its dependence on S and should be, therefore, weak. Thus, the dependence of l on T and x is generally determined by the last (exponential) factor in (12). Assuming, according to the estimations of [6], that $S \sim 10^{-13}$ cm^{-3}, $N_0 \sim 10^{22}$ cm^{-3}, and $\delta_0 \sim 10^{19}$ cm^{-3}, we can assess l_0 as ~ 155 μm.

Fig. 4 (curves 1 and 2) presents the calculated value of $\Delta\varphi = \varphi(\infty) - \varphi(0)$ as depending on x for compositionally homogeneous CMT at $T = 293$ and 345 K; these temperature values correspond to the two applied IBM techniques, namely, with cathode water cooling and without cooling, respectively. It is seen that $\Delta\varphi > 0$, therefore, the electric field at the interface between the defect layer and the conversion one hinders the diffusion of positively charged $Hg_I^{\bullet\bullet}$ atoms into the crystal. When x value is big, $\Delta\varphi$ increases with x almost linearly. When $x < 0.28$, this dependence gets weaker with x decreasing. With temperature increasing, $\Delta\varphi$ decreases, and the conversion depth l increases.

The calculated conversion depth l in vacancy-doped CMT is presented in Fig. 3. For calculations, we assumed that $\Phi = 1\cdot10^{18}$ cm^{-2} and $\Delta_{Te} = 1\cdot10^{16}$ cm^{-3}, so $l = l_r$. It is seen from the figure that the values of l_r calculated according to the proposed model agree well with those experimentally observed, if the factor l_0 in (12) is assumed to be $l_0 = 143$ μm. We should like to emphasize that the l_0 value obtained by fitting was very close to $l_0 \approx 155$ μm derived theoretically. This strongly

supports the validity of the proposed conversion mechanism. Therefore, it is the dependence of $\Delta\varphi$ on alloy composition that most probably determines the $l(x)$ dependence in compositionally uniform CMT.

The calculated dependence of the reduced conversion depth l_r, as defined by (1), on the temperature is given in Fig. 5 (curve 3). The calculations were performed for CMT with $x = 0.2$ under the assumption that $l_0 = 143$ μm. Fig. 5 (points *1* and *2*) also demonstrates the values of l_r calculated using (1) on the basis of experimental data [12] for two CMT crystals with the vacancy concentration $1 \cdot 10^{16}$ cm^{-3} (*1*) and $5 \cdot 10^{15}$ cm^{-3} (*2*) subjected to IBM at the temperatures 130, 170, 230 and 330 K, and ion fluence $\Phi = 4.5 \cdot 10^{18}$ cm^{-2}. It is obvious that, in this case, the calculated values agree well with the experimental data, too. The fact that experimentally derived values of l_r exceed those obtained by calculations by the factor of ~ 1.5, can be explained by higher IBM current density in [12] (0.6 mA/cm^2). Such current density causes strong thermal effects that mask the pure phenomenon.

We should like to emphasize that in our model the dependence of l on temperature is explained solely by the variation of the potential φ with T, while in [12] this dependence was related to the temperature dependence of the diffusion coefficient of interstitial mercury. In our model, according to (12) and (13), l does not depend on this diffusion coefficient.

The results presented in this paper do not account for the effect of the damaged layer and/or top *n*-layer with the high donor concentration. Generally speaking, these layers may affect the conversion via their effect on the potential of the electrostatic filed and by capturing mercury interstitials on radiation-induced defects.

Under the assumption that the potential of the top *n*-layer complies with the Poisson equation in the continuous approximation (6), the potential difference φ_N for electrons in the top *n*-layer and in the bulk of the conversion layer is about $(2 - 3)k_BT/e$ at $N \sim 10^{17}$ cm^{-3}, and it can strongly affect the conversion depth l. However, in reality the effective $e\varphi_N$ value should be substantially smaller due to the strong non-uniformity in the potential of the top *n*-layer of the range of few k_BT, and mercury interstitials can selectively migrate along its valleys. This non-uniformity is caused by two factors. The first of them is high density of dislocations in the damaged layer (~ 10^{13} cm^{-2} [11]); these dislocations strongly polarize the medium by their elastic field due to deformation reciprocal action. The second one is insufficient screening of the donor potential at $N_I \sim 10^{17}$ cm^{-3}; in this case $(4\pi/3)N_I r_0^3 \approx 1$, and the continuous approximation (6) is not valid for the *n*-layer. In this situation, the effective value of $e\varphi_N$ is determined not by the average value of the potential, but rather by its values along the real paths of $Hg_I^{\bullet\bullet}$ migration. For the reason, the potential of the damaged layer affects the conversion depth at $l >> 1$ μm very scarcely.

The other option for the effect of the top *n*-layer is the caption of non-equilibrium $Hg_I^{\bullet\bullet}$ on neutral radiation-induced defects in this layer. The fact that it is by this mechanism the top *n*-layer is formed is favored by the deep relaxation of its conductivity (see Fig. 1). For this relaxation, the observed variation of the carrier concentration with time is best explained by the reaction of neutralization of a doubly ionized donor by free electrons: $2e' + D^{\bullet\bullet} \rightarrow D^{\times}$.

In such a system, on one hand, one might observe a specific relay mechanism of acceleration of $Hg_I^{\bullet\bullet}$ diffusion, since when a free charged defect gets in the *n*-layer, it decreases the energy of already captured defects of the same charge sign, and stimulates the dissociation of complexes on the distance of the order of r_0. This phenomenon can only weaken the effect of the top *n*-layer on the conversion depth. On the other hand, the caption of $Hg_I^{\bullet\bullet}$ on radiation-induced defects decreases the flux of $Hg_I^{\bullet\bullet}$ in the depth of the conversion layer, which is equivalent to the decrease of the effective rate of $Hg_I^{\bullet\bullet}$ generation by the rate of surface drain generation. However, the amount of the interstitial mercury atoms captured on radiation-induced defects (~ $5 \cdot 10^{13}$ cm^{-2}, see Fig. 1), is of the same order as that of the atoms captured on the vacancies in the bulk of the conversion layer; hence, the latter effect can account only for a non-crucial l_0 renormalization.

5. Conclusions

The diffusion model of the formation of the excessive Hg source in CMT crystals subjected to IBM, proposed by the authors [6 – 8], explains all the basic features of the dependence of the conversion depth on the IBM temperature and alloy composition both quantitatively and qualitatively. This is true in relation to both compositionally homogeneous CMT crystals and for the samples with a wide bandgap protective layer. The major factor, which defines these dependences, is an electric field located at the interface between the *p*-type defect layer and the *n*-type conversion layer, as well as in the varyband region of the structures. The *p*-*n* junction field weakens the flux of Hg atoms from the source into the crystal, while the varyband region field enhances it. At small irradiation doses, the drift of charged interstitial Hg in the varyband region field leads to the linear dependence of the conversion depth on the ion dose, while the slope of this dependence becomes inversely proportional to the initial Hg vacancy concentration. The results presented in this work allow one to precisely predict and control the conversion depth in CMT crystals and epitaxial layers subjected to IBM, which is important to modern CMT-based photodetector technology.

6. Acknowledgments

These investigations were partly supported by the Ministry of Education and Science of Ukraine.

References

1. I.M. Baker, C.D. Maxey, Summary of HgCdTe 2D array technology in the UK // *J. Electron. Mater.* **30** (6), p. 682-68 (2001).
2. V.P. Ponomarenko, Cadmium mercury telluride and the new generation of photoelectronic devices // *Phys. Usp.* **46** (6), p. 629-644 (2003).
3. J.T.M. Wotherspoon, Method of manufacturing a detector device // UK Patent GB2095898 (1981).
4. K.D. Mynbaev, V.I. Ivanov-Omskii, Modification of $Hg_{1-x}Cd_xTe$ properties by low-energy ions // *Semicond.* **37** (10), p. 1127–1150 (2003).
5. C.M. Stahle and C.R. Helms, Ion sputter effects on HgTe, CdTe, and HgCdTe // *J. Vac. Sci. Technol.* **A10** (5), p. 3239-3245 (1992).
6. V.V. Bogoboyashchii, I.I. Izhnin, Mechanism for conversion of the type of conductivity in *p*-$Hg_{1-x}Cd_xTe$ crystals upon bombardment of low-energy ions // *Russ. Phys. J.* **43** (8), p. 627-636 (2000).
7. V.V. Bogoboyashchii, A.P. Vlasov, I.I. Izhnin, Mechanism for conversion of the conductivity type in arsenic-doped p-$Cd_xHg_{1-x}Te$ subject to ion etching // *Ibid.* **44** (1), p. 61–70 (2001).
8. V.V. Bogoboyashchiy, I.I. Izhnin, Mechanism for creation of the mercury diffusion source at type conductivity conversion in p-$Hg_{1-x}Cd_xTe$ under ion-beam milling // *Proc. SPIE* **5126**, p. 427-433 (2003).
9. R. Kelly, in: Proceedings of the International Conference on Ion Beam Modification of Materials **3**, p. 1465, eds. J. Gyulai, T. Lohner, E. Pasztor, Budapest, Hungary (1979).
10. R. Haakenaasen, T. Colin, H. Steen, L. Trosdahl-Iversen, Depth and lateral extension of ion milled *p-n*-junctions in $Cd_xHg_{1-x}Te$ from electron beam induced current measurements // *J. Appl. Phys.* **91** (1), p. 427-432 (2002).
11. M.A. Lunn, P.S. Dobson, Ion beam milling of $Cd_{0.2}Hg_{0.8}Te$ // *J. Cryst. Growth* **72** (2), p. 379-384 (1985).
12. E. Belas, R. Grill, J. Frank, A. Toth, P. Höschl, H. Sitter, P. Moravec, Determination of the migration energy of Hg interstitials in (HgCd)Te from ion milling experiments // *Ibid.* **159** (1-4), p. 1117-1122 (1996).
13. V.V. Bogoboyashchyy, S.A. Dvoretsky, I.I. Izhnin, N.N. Mikhailov, Yu.G. Sidorov, F.F. Sizov, V.S. Varavin, and V.A. Yudenkov, Properties of MBE $Cd_xHg_{1-x}Te$ / GaAs structures modified by ion-beam milling // *Phys. status solidi* (*c*) **1** (2), p. 355-359 (2004).
14. W.A. Beck, J.R. Anderson, Determination of electric transport properties using a novel magnetic-field-dependent Hall technique // *J. Appl. Phys.* **62** (2), p. 541-554 (1987).
15. V.V. Bogoboyashchiy, Concentration dependence of ionization of mercury vacancies in narrow gap $Hg_{1-x}Cd_xTe$ crystals // *Cond. Media & Interfaces* **3** (1), p. 28-33 (2001).
16. V.V. Bogoboyashchyy, K.R. Kurbanov, Reaction constants for main cationic native defects in narrow-gap $Hg_{1-x}Cd_xTe$ crystals // *J. Alloys and Compounds* **371** (1-2), p. 97-99 (2004).
17. V. Bogoboyashchiy, Interconsistent band structure of narrow-gap $Hg_{1-x}Cd_xTe$ alloys obtained with taking into account far band influence // *Proc. SPIE* **3486**, p. 325-335 (1997).
18. A. Moritani, K. Taniguchi, C. Hamaguchi, J. Nakai, Electroreflectance study of $Cd_xHg_{1-x}Te$ // *J. Phys. Soc. Jpn* **34** (1), p. 79-88 (1973).
19. V.V. Bogoboyashchyy, Density of heavy hole states of $Hg_{1-x}Cd_xTe$ in an isotropic nonparabolic approximation by exact measurements of electron concentration // *Semiconductor Physics, Quantum Electronics & Optoelectronics* **4** (4), p. 273-277 (2001).